Catalysis Science & Technology

PAPER

View Article Online
View Journal | View Issue

Cite this: *Catal. Sci. Technol.*, 2014, 4, 531

Assessing the surface modifications following the mechanochemical preparation of a Ag/Al_2O_3 selective catalytic reduction catalyst

Kathryn Ralphs,[a] Carmine D'Agostino,[b] Robbie Burch,[a] Sarayute Chansai,[a] Lynn F. Gladden,*[b] Christopher Hardacre,*[a] Stuart L. James,*[a] Jonathan Mitchell[b] and Sarah F. R. Taylor[a]

Received 19th November 2013,
Accepted 3rd December 2013

DOI: 10.1039/c3cy00945a

www.rsc.org/catalysis

The surface modification of a mechanochemically prepared Ag/Al_2O_3 catalyst compared with catalysts prepared by standard wet impregnated methods has been probed using two-dimensional T_1–T_2 NMR correlations, H_2O temperature programmed desorption (TPD) and DRIFTS. The catalysts were examined for the selective catalytic reduction of NO_x using *n*-octane in the presence and absence of H_2. Higher activities were observed for the ball milled catalysts irrespective of whether H_2 was added. This higher activity is thought to be related to the increased affinity of the catalyst surface towards the hydrocarbon relative to water, following mechanochemical preparation, resulting in higher concentrations of the hydrocarbon and lower concentrations of water at the surface. DRIFTS experiments demonstrated that surface isocyanate was formed significantly quicker and had a higher surface concentration in the case of the ball milled catalyst which has been correlated with the stronger interaction of the *n*-octane with the surface. This increased interaction may also be the cause of the reduced activation barrier measured for this catalyst compared with the wet impregnated system. The decreased interaction of water with the surface on ball milling is thought to reduce the effect of site blocking whilst still providing a sufficiently high surface concentration of water to enable effective hydrolysis of the isocyanate to form ammonia and, thereafter, N_2.

1. Introduction

Recently the trend in lean-burn NO_x reduction for mobile applications has been towards ammonia Selective Catalytic Reduction (SCR), or NO_x Storage and Reduction (NSR), or a combination of SCR and NSR. Nevertheless, selective catalytic reduction using an on-board hydrocarbon fuel, Hydrocarbon Selective Catalytic Reduction (HC-SCR), would offer significant benefits if catalysts with sufficient low temperature activity could be developed. Silver-based catalysts appear to be the most promising but are relatively inactive at temperatures below about 350 °C.[1–18] Various modifications to the standard wet impregnation preparation technique have been investigated with a view to improving the activity of alumina-supported Ag catalysts. For example, co-precipitation,[10] sol–gel processes[11–15] and hydrolysis[16–18] methods have been reported but, to date, the highest activity catalysts prepared by these methods are produced *via* wet impregnation from aqueous solutions using $AgNO_3$ as the Ag precursor. In addition, the effect of the addition of hydrogen has been extensively studied.[19–29] A strong increase in the activity of the catalyst was observed on addition of hydrogen, for example Burch and co-workers[19,20] observed a decrease in the light off temperature for a wet impregnated Ag/Al_2O_3 catalyst from 410 to 195 °C.

Mechanochemical treatment of solid materials by ball milling and related techniques has a long history in the context of inorganic materials synthesis,[30–34] and has recently been investigated for organic[35] and metal–organic synthesis.[36] Its use in preparing heterogeneous catalysts has recently been reviewed and showed significant increases in activity could be achieved for a wide range of reactions including deNO_x, CO oxidation and VOC removal.[37] Recently, we showed[38] that Ag/Al_2O_3 catalysts could be prepared simply by ball milling alumina and a Ag precursor, for example Ag_2O or Ag metal. These materials were highly active for the HC-SCR of NO_x even in the low temperature range, showing light-off temperatures (*i.e.*, temperature at which the conversion is 50%) below 300 °C, with the catalyst prepared using silver oxide resulting in a light-off temperature of 240 °C. The increased activity was not correlated to an increase in the BET

[a] *Centre for the Theory and Application of Catalysis, CenTACat, School of Chemistry and Chemical Engineering, Queen's University, Belfast, BT9 5AG, UK. E-mail: c.hardacre@qub.ac.uk, s.james@qub.ac.uk*
[b] *Department of Chemical Engineering and Biotechnology, University of Cambridge, Pembroke Street, Cambridge CB2 3RA, UK. E-mail: lfg1@cam.ac.uk*

surface. In addition, transmission electron microscopy and UV-Vis studies of the impregnated and ball milled catalysts revealed a similar particle size distribution of the silver.[38]

In this paper, the mechanochemically prepared Ag/Al_2O_3 catalyst was examined for the HC-SCR of NO_x in the presence of hydrogen to assess whether the activity could be further improved. In addition, *in situ* diffuse reflectance infra-red spectroscopy (DRIFTS) and NMR have been used to compare the changes in the surface interactions due to the mechanochemical processing. T_1–T_2 NMR two-dimensional correlations have been used[39] to investigate surface interactions of two important species involved in the SCR reaction, *n*-octane and water, within Al_2O_3 supports and Ag/Al_2O_3 catalysts prepared by standard wet impregnation and by the ball milling method. NMR relaxometry has been widely used to characterise surface interactions in porous materials[40–43] and has been very recently applied to heterogeneous catalysts[44,45] and molecular dynamics.[46] In particular, the use of the T_1/T_2 ratio has the advantage of being independent of surface-to-volume ratio of the pores.[47] Therefore, such a ratio will only be dependent on the surface properties and not upon the geometrical characteristics of the pore structure. Hence, it allows us to compare materials with different pore structures and gives us a direct correlation with the surface interactions and how the ball milling process affects these. This is because the interactions are independent of surface-to-volume ratio. In addition, this makes the method also more robust to effects deriving from a different "filling" of the pore volume by different liquids. However, we anticipate that in the present work, the pores are small (order of few to tens of nanometers) in all samples and so the observed relaxation times are surface-dominated in all cases. If the volume of liquid dropped below monolayer coverage, then we might see a change due to different volume within the pore space, but this is not relevant to the saturated systems used here.

The aim of this work is to gain a better understanding how the ball milling process can improve the SCR activity and can change the NMR relaxation properties of the *n*-octane and water chemical species within the catalysts, from which it is possible to infer the strength of surface interaction with the catalytic surface and hence gain further insights into the understanding of the catalytic performance.

2. Experimental

2.1 Catalyst preparation

Ag/Al_2O_3 catalyst, denoted as Ag_2O_BM, was prepared by ball milling using Ag_2O as the Ag precursor. The Ag_2O precursor (0.0438 g) (99.99%, Sigma Aldrich) and 2.00 g of as received γ-Al_2O_3 (Grace-Davison, BET surface area = 261 m^2 g^{-1}) were well-mixed using a spatula before being placed into a 500 cm^3 sintered aluminium oxide grinding jar with seven 10 mm diameter sintered alumina grinding balls. Milling was performed in a Retsch PM100 Planetary Ball Mill at a rotation speed of 150 rpm for 1 h. A standard Ag/Al_2O_3 catalyst, denoted as Ag_STD, was prepared by wet impregnation using 0.022 M $AgNO_3$ solution to obtain a silver loading of 2 wt% on the same γ-Al_2O_3 as used for the ball milled sample. The catalyst was then dried in an oven overnight at 100 °C. The resulting Ag_2O_BM and Ag_STD catalysts were calcined at 650 °C for 2 h. To prepare the ball milled alumina blank, the same procedure was used without the silver oxide present. The Ag content of the catalysts was determined by the inductively coupled plasma method and determined to be approximately 2 wt% Ag. The BET specific surface areas of the catalysts were 235 m^2 g^{-1} and 258 m^2 g^{-1} for Ag_2O_BM and Ag_STD, respectively. As reported previously, for both catalysts under reaction conditions, the silver was found to be in the form of both isolated Ag^+ ions and $Ag_n^{\delta+}$ ($n \leq 8$) clusters using diffuse reflectance UV-vis spectroscopy.[38]

2.2 Catalytic activity tests

Typically, the catalytic activity tests over Ag/Al_2O_3 catalysts were carried out in a fixed-bed flow reactor system, consisting of a quartz reactor tube. The catalysts were held in place between plugs of quartz wool and a K-type thermocouple was placed in the centre of the catalyst bed. Each of the gases in the feed system was controlled individually by mass flow controllers, while *n*-octane and water vapour were introduced to the system by means of separate saturators with Ar as a carrier gas. The *n*-C_8H_{18} saturator was placed in an ice/water bath and the H_2O saturator temperature was controlled using a thermostatic bath. All the lines following the water saturator were trace heated to prevent condensation.

The feed gas stream consisted of 720 ppm NO; 4340 ppm *n*-C_8H_{18} (as C_1); 4.3% O_2, 7.2% H_2O (when added); 7.2% CO_2; 0.72% H_2 and Ar balance was introduced to the reactor which was heated from 150 to 600 °C and then back down to 150 °C stepwise at 50 °C intervals dwelling at each temperature for 40 min in order to obtain steady state conditions. The total gas flow rate was 276 cm^3 min^{-1} over 276 mg of catalyst which was sieved to obtain particle size of 250–450 μm. The space velocity for all catalytic tests was 60 000 cm^3 g^{-1} h^{-1} (calculated using the total gas flow rate divided by the amount of the catalyst used in the activity test). The inlet and outlet NO_x concentrations were determined by a Signal 4000VM series chemiluminescence detector. The oxidation of *n*-octane was measured online using a Bruker Tensor 27 IR spectrometer, fitted with a gas cell of volume 190 cm^3.

All the activity data was measured during the decreasing temperature ramp. Using this method, the activity remained constant once the desired temperature had been reached and the conversions were calculated from an average of outlet NO_x readings at each temperature. In contrast, measurements made on ramping the temperature up showed that steady state was reached after 15–20 min although it should be noted that the values between the two ramps once steady state had been reached only showed small variations. The time to reach steady state on increasing the temperature was associated with a dip in the NO_x concentration once the temperature had been reached; however, this is not due to reaction but adsorption of the NO_x.

2.3 NMR relaxometry

Four different samples were used for the experiments namely as received γ-Al_2O_3 (Al_2O_3_STD), ball milled γ-Al_2O_3 (Al_2O_3_BM), wet impregnated 2% Ag/γ-Al_2O_3 (Ag_STD) and ball milled 2% Ag/γ-Al_2O_3 (Ag_2O_BM). NMR experiments were performed in a Bruker DMX 300 operating at a ^1H frequency of 300.13 MHz. NMR relaxation experiments were performed using a T_1–T_2 pulse sequence, which comprises a saturation recovery measurement to encode T_1 (using a comb of 90° pulses) followed by a Carr–Purcell Meiboom–Gill (CPMG) echo train of 180° pulses to encode T_2. The sequence is schematically shown in Fig. 1. The T_1 recovery interval, t_{delay}, was varied logarithmically between 1 ms and 5 s in 32 steps. The echo spacing between the 180° pulses of the CPMG was set to 250 μs. More details of the pulse sequence used are reported elsewhere.[39,41,48]

Samples were prepared by soaking the catalytic material in *n*-octane or water for at least 24 h. The wet catalyst was then removed from the liquid, placed on a pre-soaked filter paper (with the liquid *n*-octane or water) in order to remove excess external liquid and finally placed into the NMR tube. To ensure a saturated atmosphere in the NMR tube, hence minimising errors due to evaporation of volatile liquids, a small amount of pure liquid was placed onto absorbed filter paper, which was then placed in the cap of the NMR tube. All the NMR measurements were performed at atmospheric pressure and 20 °C using 5 mm NMR glass tubes.

2.4 H_2O temperature-programmed desorption (TPD)

The H_2O-TPD measurements were performed to investigate the adsorption properties of water on the supports (Al_2O_3_STD and Al_2O_3_BM) and the Ag catalysts (Ag_STD and Ag_2O_BM). In each of the experiments, approximately 50 mg of fresh sample was used and pre-treated in Ar at a flow rate of 100 cm^3 min^{-1} for 30 min at 300 °C. The catalyst was then cooled down to 50 °C where a gas mixture of 0.5% H_2O–1% Kr/Ar with the same flow rate was introduced for one hour. Water vapour was introduced to the system by means of a saturator with Ar flow as a carrier gas. The H_2O saturator temperature was carefully controlled at 10 °C using a Grant™ GD120 thermostatic bath. Following H_2O adsorption, the catalyst was purged by 1% Kr/Ar flow at the total rate of 100 cm^3 min^{-1} for 30 min to remove any weakly bound H_2O. Finally, the temperature was ramped at a rate of 10 °C min^{-1} up to 700 °C under 1% Kr/Ar flow. Kr was used as an internal standard for quantification. The desorbed H_2O was monitored by a Hiden quadrupole mass spectrometer.

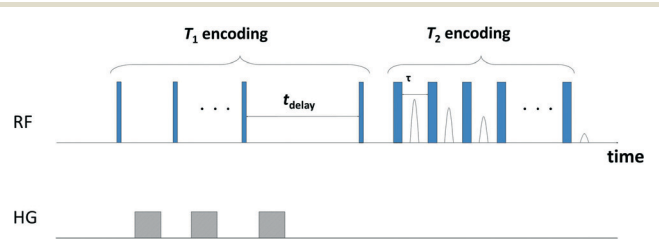

Fig. 1 T_1–T_2 NMR pulse sequence. The thin and thick vertical bars represent 90° and 180° radiofrequency (RF) pulses, respectively. T_1 relaxation is encoded in the variable time t_{delay}. T_2 relaxation is encoded in the train of *n* 180° pulses. A single data point is acquired at the centre of each echo time, τ. The cross-hatched patterns (HG) represent homospoil magnetic field gradients.

2.5 DRIFTS analysis

In situ DRIFTS measurements were performed using a Bruker Vertex 70 FTIR spectrometer equipped with a liquid N_2-cooled detector. In a typical experiment, 25 mg of catalyst was placed in a ceramic crucible in the DRIFTS cell.

Prior to the experiments, the catalyst was pre-treated by heating in 5% O_2/Ar with a total flow rate of 100 cm^3 min^{-1} up to 300 °C for 1 h and then cooled down in flowing Ar to 250 °C. The IR spectrum of the Ag/Al_2O_3 catalyst at 250 °C under flowing Ar was taken as a background. Two 4-way VICI valves were installed to allow us to switch between two gas mixtures. The DRIFTS was used to examine the relative surface concentrations of isocyanate on each catalyst. Therefore, each catalyst was exposed to C_8H_{18} + O_2 gas feed at 250 °C for 30 min and followed by a flowing NO + O_2 feed for 10 min. In all cases, the *in situ* DRIFTS spectra were recorded with a resolution of 4 cm^{-1} and with an accumulation of 16 scans every 10 s. The DRIFTS spectra were analyzed by the OPUS software. The concentrations of the reactants used were 720 ppm NO + 4.3% O_2 and 4340 ppm (as C_1) *n*-C_8H_{18} + 4.3% O_2 and Ar balance. The total flow rate was 100 cm^3 min^{-1}.

3. Results and discussion

Fig. 2 shows a comparison of the NO_x conversion of the most active ball-milled Ag catalyst (Ag_2O_BM) with that of a conventional wet impregnated Ag/Al_2O_3 catalyst (Ag_STD) in the presence and absence of H_2. For the purpose of comparison, we take as the reference point the light-off temperature which we define as the temperature for 50% NO_x conversion. Fig. 2

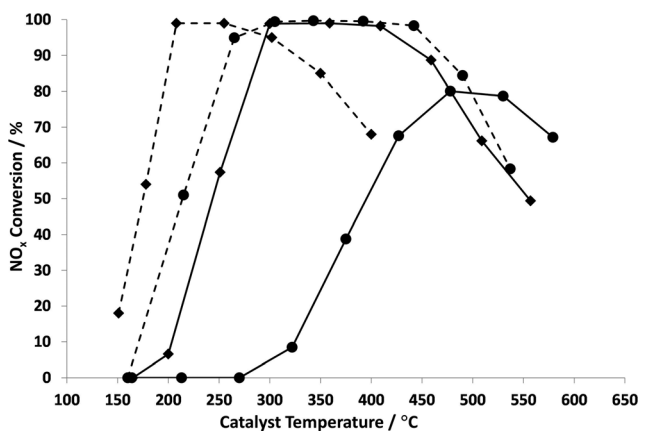

Fig. 2 NO_x conversion as a function of catalyst temperature for the SCR of NO_x reaction with *n*-octane over Ag_STD (●) and Ag_2O_BM (♦) catalysts in the absence (solid) and the presence (dashed) of H_2. Feed stream: 720 ppm NO, 4340 ppm (as C_1) *n*-C_8H_{18}, 4.3% O_2, 7.2% CO_2, 7.2% H_2O, 0.72% H_2 and Ar balance. Space velocity: 60 000 cm^3 g^{-1} h^{-1}.

shows that the ball-milled catalyst has a light-off temperature of only about 240 °C whereas the wet impregnated catalyst has a light-off temperature of about 370 °C in the absence of hydrogen, in agreement with previously reported results.[38] In the presence of 0.72% hydrogen, the light-off temperature was reduced from 240 °C (without H_2) to 165 °C (with H_2) for Ag_2O_BM and from 370 °C (without H_2) to 180 °C (with H_2) for Ag_STD. In addition, 100% NO_x conversion was obtained at 220 °C and 298 °C for the ball milled and wet impregnated catalysts, respectively, compared with ~300 °C for the ball milled catalyst in the absence of hydrogen and 80% conversion at ~450 °C for the Ag_STD catalyst. Although a wider range of operational temperatures is observed for Ag_STD than Ag_2O_BM, the activity of the ball milled catalyst is significant as these results show the lowest temperature activity for *n*-octane-SCR reported up to date, albeit in the presence of hydrogen.[19,20] The effect of hydrogen is consistent with previous studies on HC-SCR over silver catalysts.[8,21-23] It is now generally accepted that the role of the hydrogen is to modify the chemical reactions rather than to significantly change the nature of the silver under reaction conditions.

Moreover, the SCR activity with *n*-octane over Ag catalysts in the absence of water was investigated and presented in Fig. 3. For both Ag_STD and Ag_2O_BM catalysts, it is clearly seen that the conversion of NO_x was suppressed when there was no water added into the SCR feed. This is consistent with previous work by Shimizu *et al.*[17] This has been attributed to the possibility that, with water in the feed, the deposition of carbonaceous species such as carboxylates and carbonates is reduced.[17] However, it is also noted that water is necessary for the hydrolysis of NCO species formed during the reaction to form nitrogen. These have been reported to be important intermediates in the SCR reaction over Ag catalysts and thus the presence of water is critical in the reaction mechanism.[8,23]

It is well known that both the activation of the hydrocarbon and presence of water are critical for the HC-SCR of NO_x over Ag based catalysts,[1,3,8,17,49,50] therefore, due to the fact that there is a significant difference in NO_x conversion profile and operational temperature window for the Ag_2O_BM and Ag_STD catalysts, the interactions of *n*-octane and water were examined on each catalyst using two-dimensional T_1–T_2 NMR.

The two-dimensional T_1–T_2 NMR correlation maps for the pure Al_2O_3 samples are shown in Fig. 4 in the presence of water or *n*-octane. In all cases, a single peak is observed, with water giving rise to broader peaks due to the greater uncertainty involved in fitting the exponential decay function for short T_2 relaxation times. The position of the dashed diagonal in each plot is determined from the maximum peak intensity and corresponds to the T_1/T_2 ratio. This ratio is considered to be an indicator of the strength of interaction between the liquid and the solid surface. An increase in the magnitude of T_1/T_2 indicates an increase in the strength of the surface interaction of a given molecular species with the surface.[41] Water in Al_2O_3_STD exhibits T_1/T_2 = 63, whereas in Al_2O_3_BM it gives T_1/T_2 = 57. The values for *n*-octane are T_1/T_2 = 31 in Al_2O_3_STD and T_1/T_2 = 38 in Al_2O_3_BM. The significant difference between the T_1/T_2 ratios for water and those for *n*-octane clearly indicate that water has a stronger interaction with the alumina surface compared with *n*-octane. This result is expected given the polarity and ability of water to form hydrogen bonds with the surface hydroxyl groups of the Al_2O_3. Comparing the two alumina samples, small but significant changes are observed for each liquid. Water has a lower strength of interaction with Al_2O_3_BM compared with Al_2O_3_STD; conversely, *n*-octane has a higher strength of interaction with Al_2O_3_BM. Although these differences in the T_1/T_2 ratios are not large, they are reproducible and greater than the error associated with determining the individual T_1/T_2 ratios from the correlation plots (see Fig. 6,

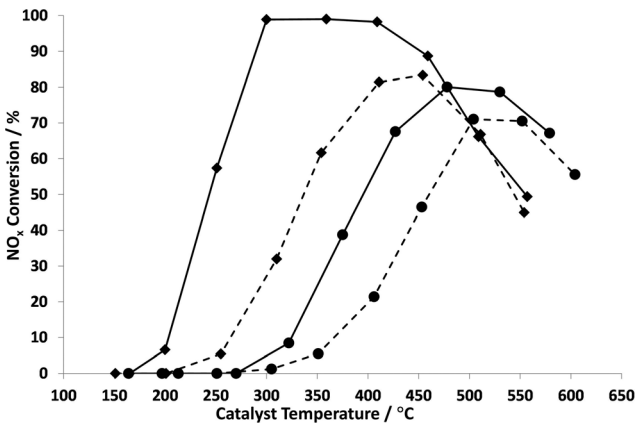

Fig. 3 NO_x conversion as a function of catalyst temperature for the SCR of NO_x reaction with *n*-octane over Ag_STD (●) and Ag_2O_BM (♦) catalysts in the presence (solid) and the absence (dashed) of H_2O. Feed stream: 720 ppm NO, 4340 ppm (as C_1) *n*-C_8H_{18}, 4.3% O_2, 7.2% CO_2, 7.2% H_2O (when added), and Ar balance. Space velocity: 60 000 cm^3 g^{-1} h^{-1}.

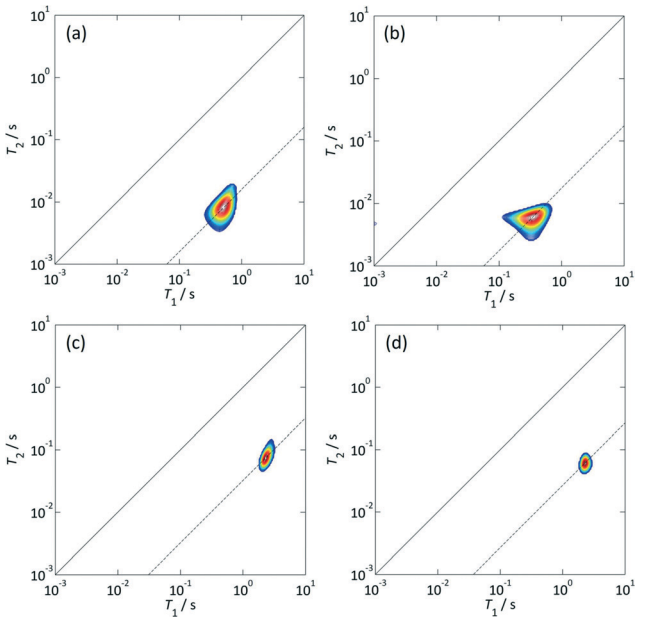

Fig. 4 T_1/T_2 of: (a) water in Al_2O_3_STD; (b) water in Al_2O_3_BM; (c) *n*-octane in Al_2O_3_STD; (d) *n*-octane in Al_2O_3_BM.

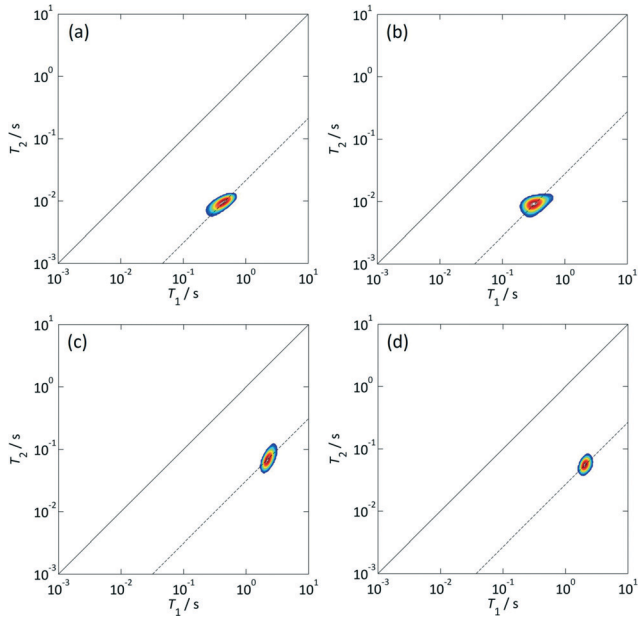

Fig. 5 T_1/T_2 of: (a) water in Ag_STD; (b) water in Ag_2O_BM; (c) *n*-octane in Ag_STD; (d) *n*-octane in Ag_2O_BM.

error bars). Therefore, we infer that the ball milling process changes the properties, specifically the affinity of the Al_2O_3 surface towards water and *n*-octane.

The T_1–T_2 correlations for water or *n*-octane in the Ag/Al_2O_3 catalysts are shown in Fig. 5. The ball milling decreases the T_1/T_2 of water within the catalyst: water in Ag_STD gives T_1/T_2 = 47, and in Ag_2O_BM gives T_1/T_2 = 35. Conversely, the ratio for *n*-octane increases with ball milling from T_1/T_2 = 32 in Ag_STD to T_1/T_2 = 38 in Ag_2O_BM. This trend in T_1/T_2 observed for the catalysts is similar to that observed for the Al_2O_3 supports.

The T_1/T_2 ratios are summarised in Fig. 6. The difference in the T_1/T_2 values between water and *n*-octane for the different samples can be seen in terms of competitive interaction strength. In the context of the catalytic data presented here it is the observation that the reduction in the interaction strength of water compared with *n*-octane with the ball milled sample compared with the conventionally prepared sample that is of particular significance.

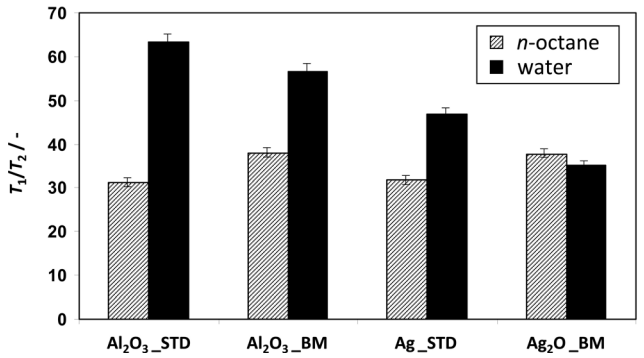

Fig. 6 Summary of T_1/T_2 of water and *n*-octane in Al_2O_3 and Ag/Al_2O_3 samples. Error bars are also reported.

It is noted that paramagnetic species might affect both T_1 and T_2 relaxation times. However, these oxides are known to be free of paramagnetic species. Even in the case of traces of paramagnetic impurities, these would be the same in all samples and, therefore, would affect the relaxation times in a similar manner for both *n*-octane and water. Hence, this cannot be the determining factor in the differences in T_1/T_2 observed. Indeed, the ball mill used in this work has sintered alumina grinding balls, which excludes the possibility of contamination from introducing, for example, paramagnetic iron particles during the ball milling process, which could, for instance, be present if steel balls were used in the milling process.

In addition to NMR study, the interaction of water on the Al_2O_3 supports and Ag catalysts was probed using temperature programmed desorption. The concentration profiles of desorbed H_2O as a function of catalyst temperature are illustrated in Fig. 7. Fig. 7a shows that there is a difference in the desorption profiles and the amount of desorbed H_2O between Al_2O_3_STD and Al_2O_3_BM. The concentration of H_2O on Al_2O_3_STD peaks at about 135 °C whereas Al_2O_3_BM sample shows two desorption features at 112 and 215 °C. The calculated amount of desorbed H_2O is 457.0 and 343.7 μmol g_{cat}^{-1} for Al_2O_3_STD and Al_2O_3_BM, respectively. For the Ag_STD and Ag_2O_BM catalysts, similar profiles for the desorbed H_2O

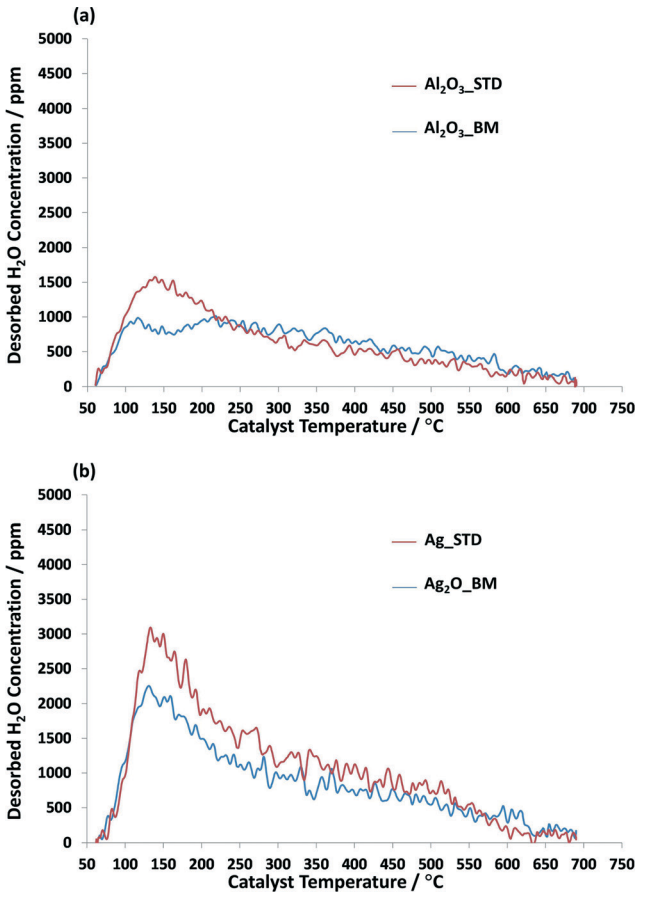

Fig. 7 TPD profiles of H_2O desorption on (a) Al_2O_3 supports and (b) Ag/Al_2O_3 catalysts.

were observed, in which water starts to desorb at 55 °C and peaks at about 130 °C before gradually declining as the temperature was raised up to 700 °C. The amount of H_2O desorbed is found to be 653.3 and 443.5 μmol g_{cat}^{-1} for Ag_STD and Ag_2O_BM samples, respectively. As shown in Fig. 7, the amount of water desorbed on the ball-milled support and ball-milled Ag catalyst is significantly lower than desorbed from the received support and wet-impregnated Ag catalyst. It should be noted that, whilst a small drop in the BET surface area is found for the ball milled catalysts compared with the as received alumina and the wet impregnated prepared silver catalyst of ~10%[38] and will contribute to the lower amounts of water desorbed, the extent of the decrease found in the TPD is much higher. Therefore, a smaller number of adsorption sites for the water is found for the ball-milled samples compared with the standard catalyst/support.

The ball milling is, therefore, inducing surface changes of the samples as observed by both TPD and NMR measurements. It is known that the absolute relaxation times depend on the density of adsorption sites, which is manifested as a weak dependence in T_1/T_2.[51] However, this sensitivity of T_1/T_2 to adsorption site density can only be detected when the surface chemistry of the system being studied is the same. For example, in previous work on water in porous plasters, small changes in T_1/T_2 were related to variations in the number of surface sites; this interpretation was appropriate as the type of surface adsorption sites did not change between samples.[40] In this work, the TPD results presented suggests that the ball milling process is decreasing the number of adsorption sites for water molecules, hence in the discussion made above, this may be expected to affect the T_1/T_2 values for water, which are lower on the ball milled samples. However, a quantitative analysis is not sufficient to explain the NMR data. Indeed, NMR relaxation results also show that for the ball milled samples there is a consistent increase in the T_1/T_2 values for the hydrocarbon, which implies also qualitative changes of adsorption sites. This suggests that the ball milling changes the properties of some of the adsorption sites, which results in a lower affinity for water and higher affinity for the hydrocarbon. In summary, there is a quantitative but also a qualitative change of the surface due to ball milling, which increases the affinity of the surface towards the hydrocarbon relative to water. As shown below, the DRIFTS results and the activation barrier for *n*-octane oxidation are also in line with such findings.

It has to be highlighted that the details of such changes at this stage are not yet fully elucidated and more work is required to obtain more detailed insights. However, the current results show evidence that such changes are occurring, which support the hypothesis made in previous work.[38]

It has to be noted that such NMR relaxation measurements aims at characterizing the surface affinity of the materials for the different species and are carried out at room temperature. It is clear that reaction conditions are different in terms of temperature and complexity of all the reaction species involved. NMR relaxation measurements under such conditions would be challenging and not necessarily feasible. However, the measurements reported here offer more reliability, are easier to interpret and yet give a good indication on surface properties of those materials; hence, they can be used to help understand the catalytic data, especially when combined with the other methods used in this work.

To correlate with the NMR measurements, *in situ* DRIFTS was used to examine the relative amounts and rates of formation of isocyanate as a function of preparation method. It is now widely accepted[2,5-8,12,13,21–29,52–55] that the surface NCO species is only observed when the catalyst is active and that it is probably a key intermediate in the HC-SCR reaction on Ag/Al_2O_3 catalysts. In order to examine the NCO formation on each catalyst (Ag_2O_BM and Ag_STD), both Ag catalysts were exposed to C_8H_{18} + O_2 for 30 min at 250 °C and the species monitored using DRIFTS. This allowed the active/activated $C_xH_yO_z$ species to be adsorbed on the catalyst. Subsequently, a NO + O_2 mixture was fed over the pre-treated Ag catalysts. It should be noted that these experiments were conducted in the absence of water to prevent the fast hydrolysis of surface NCO. The results are shown in Fig. 8.

From Fig. 8, after 30 min reaction under C_8H_{18} + O_2 conditions at 250 °C, a number of overlapping IR bands are observed below 1800 cm^{-1} due to the partial oxidation of *n*-octane. These species include carboxylates, acetates and formates.[5,12,13,21,22,24–29,52] IR bands in the –CH– stretching region between 3100 and 2800 cm^{-1} were also observed and assigned to *n*-octane in the gas phase as well as adsorbed hydrocarbon species.[3,12,13,21,22,52] When replacing the C_8H_{18} + O_2 with the NO + O_2 feed, it is observed that the IR bands between 3100 and 2800 cm^{-1} decreased

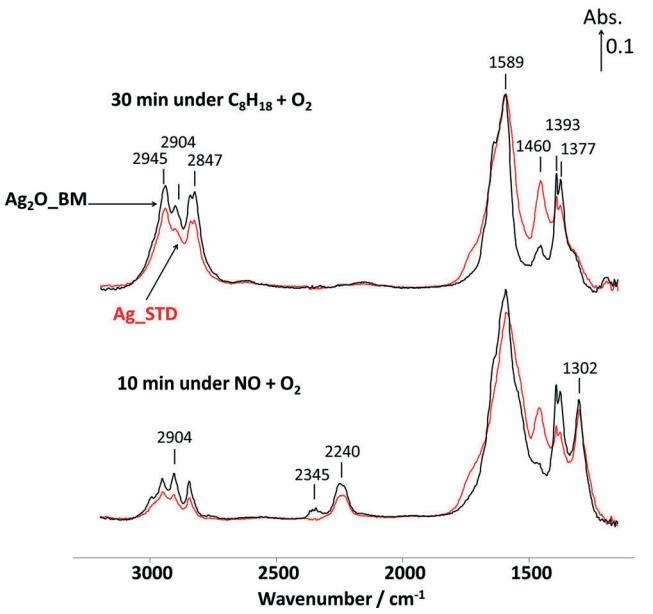

Fig. 8 *In situ* DRIFT spectra on Ag catalysts recorded at 250 °C under C_8H_{18} + O_2 and NO + O_2 conditions at 250 °C. Feed conditions: 720 ppm NO, 4340 ppm (as C_1) *n*-C_8H_{18}, 4.3% O_2, and Ar balance.

significantly and the NCO was formed shown by the band at 2240 cm^{-1} from the reaction between partially oxidized $C_xH_yO_z$ and NO_x. The appearance of the IR band at 1302 cm^{-1} is due to NO_x adsorption under NO + O_2 gas feed. In comparison with Ag_STD, the DRIFTS spectra observed on Ag_2O_BM sample revealed that there was a small peak observed at 2345 cm^{-1}, attributed to both adsorbed and gas phase CO_2 being formed from oxidation of *n*-octane.

Fig. 9 shows the dynamic change in the concentration of the NCO species on Ag_2O_BM and Ag_STD catalysts after switching in the NO + O_2 feed. It is clearly seen that the integrated area of the NCO band on Ag_2O_BM is significantly higher than that found over the Ag_STD catalyst over the entire time of the experiment. In addition, the initial rate of NCO formation on Ag_2O_BM is faster than on Ag_STD.

In order to clarify which reactions are affected by the different preparation methods, the activation barriers for the Ag_STD and Ag_2O_BM catalysts were measured for both the activation of the hydrocarbon and the reduction of the NO_x. Fitting the deNO_x reaction rate data in the kinetically controlled zone to the Arrhenius equation provides the pre-exponential factor and the activation energies. The apparent activation energy calculated from the rate of NO_x conversion (<15% conversion) for NO_x reduction on Ag_2O_BM and Ag_STD were found to be 52.7 (±3.5) and 64.2 (±3.4) kJ mol^{-1}, respectively. These may be compared with the barriers determined by Shimizu *et al.*[18] for the SCR of NO_x with *n*-hexane on 2 wt% Ag/Al_2O_3 catalyst of 67 kJ mol^{-1} for the NO reduction. This increase in barrier is consistent with the decreased activity shown using *n*-hexane *versus* *n*-octane due to the increased stability of the shorter hydrocarbon with respect to oxidation. In addition, the activation barrier for *n*-octane conversion (<15% conversion) was also calculated and found to be 45.7 (±3.8) and 57.1 (±4.5) kJ mol^{-1} for Ag_2O_BM and Ag_STD, respectively. The apparent activation barriers determined indicate that the ball milled catalyst can activate the hydrocarbon more easily than for the wet impregnated sample; however, as the barrier for both catalysts is lower than found for the NO_x reduction, it indicates that a subsequent step, for example the interaction of the NO_x with the activated hydrocarbon to form NCO may be rate determining.

The NMR, together with the TPD results, show a decreased interaction of water and an increased interaction of the hydrocarbon with the surface which may result in the decreased activation barrier for *n*-octane activation and will increase the surface concentration of hydrocarbon. Whilst this is important as the precursor to the formation of NCO an increase in the *n*-octane interaction alone would not necessarily lead to higher NO_x activity. The presence of water is also important as it provides a hydrolysis route for the decomposition of the isocyanate intermediate to form ammonia and carbon dioxide and subsequently nitrogen.[8,23,52–55] It should be noted that, at the high water concentrations employed herein, although the hydrolysis step is important to complete the catalytic cycle and form N_2, it is unlikely that this step is rate determining. Water can, however, also act as a poison for the reaction if present at too high a concentration by site blocking preventing the adsorption of both *n*-octane and NO.[17,49,50] In the case of the ball milled catalyst, the interaction of *n*-octane is found to be increased relative to the wet impregnated catalyst whereas the opposite is true in the case of water. This is consistent with the surface of the ball milled catalyst increasing the rate of NCO formation, due to increased *n*-octane at the surface, whilst maintaining sufficient surface concentration of water for efficient hydrolysis. In the case of the wet impregnated catalyst both the *n*-octane concentration will be lower and the water concentration higher leading to reduced NCO formation and potentially increased site blocking by water hence the lower activity observed.

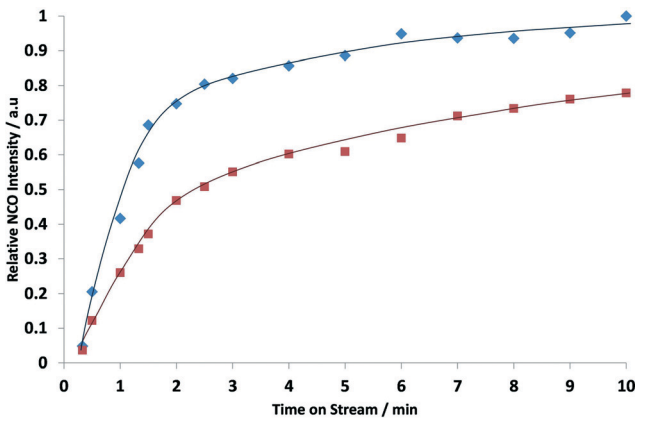

Fig. 9 Relative NCO intensity to the highest integrated peak area of NCO corresponding to Fig. 8 obtained from the integrated area of the DRIFT band at 2240 cm^{-1} under flowing NO + O_2 at 250 °C. Prior to the measurement, both Ag_STD (■) and Ag_2O_BM (♦) catalysts were pre-treated under C_8H_{18} + O_2 for 30 min at 250 °C. Feed conditions: 720 ppm NO, 4340 ppm (as C_1) *n*-C_8H_{18}, 4.3% O_2, and Ar balance. The lines provide a guide for the eye.

4. Conclusions

The work presented, herein, highlights that highly active Ag catalysts for NO_x reduction by hydrocarbons on Ag/Al_2O_3 catalysts can be prepared by ball milling Ag_2O with Al_2O_3 support. When compared with conventionally prepared wet-impregnated catalysts, the ball milled catalyst lowered the reaction temperature for NO_x reduction with *n*-octane by ~130 °C. In addition, in the presence of H_2, the lowest NO_x reduction temperature was observed, to date. Two-dimensional T_1–T_2 NMR correlation experiments and water TPD measurements coupled with *in situ* DRIFTS analysis has indicated that the active sites on the ball milled Ag catalyst increase the formation of the intermediate NCO species by increasing the hydrophobicity of both the support and catalyst. In the case of the ball milled catalyst, the interaction of water is reduced whilst the *n*-octane is enhanced which provides a balance between sufficient water to hydrolyse the NCO and yet not to act as a site blocker for NO or the hydrocarbon. This concentration change coupled with the lower activation barrier for *n*-octane activation found for the ball milled material may be the cause

of the increased activity of this catalyst compared with the wet impregnated material.

Acknowledgements

We gratefully acknowledge funding for this work from the Department of Education and Leaning in Northern Ireland and the CASTech grant (EP/G012156/1) from the EPSRC.

References

1 K. A. Bethke and H. H. Kung, *J. Catal.*, 1997, **172**, 93.
2 R. Burch, J. P. Breen and F. C. Meunier, *Appl. Catal., B*, 2002, **39**, 283.
3 A. Iglesias-Juez, A. B. Hungría, A. Martínez-Arias, A. Fuerte, M. Fernándezcía, J. A. Anderson, J. C. Conesa and J. Soria, *J. Catal.*, 2003, **217**, 310.
4 E. F. Iliopoulou, A. P. Evdou, A. A. Lemonidou and I. A. Vasalos, *Appl. Catal., A*, 2004, **274**, 179.
5 J. Wang, H. He, Q. Feng, Y. Yu and K. Yoshida, *Catal. Today*, 2004, **93–94**, 783.
6 L.-E. Lindfors, K. Eränen, F. Klingstedt and D. Y. Murzin, *Top. Catal.*, 2004, **28**, 185.
7 H. He and Y. Yu, *Catal. Today*, 2005, **100**, 37.
8 K. Shimizu and A. Satsuma, *Phys. Chem. Chem. Phys.*, 2006, **8**, 2677.
9 V. Demidyak, C. Hardacre, R. Burch, A. Mhadeshwar, D. Norton and D. Hancu, *Catal. Today*, 2011, **164**, 515.
10 X. She and M. Flytzani-Stephanopoulos, *J. Catal.*, 2006, **237**, 79.
11 K. Takagi, T. Kobayashi, H. Ohkita, T. Mizushima, N. Kakuta, A. Abe and K. Yoshida, *Catal. Today*, 1998, **45**, 123.
12 A. Sultana, M. Haneda, T. Fujitani and H. Hamada, *Catal. Lett.*, 2007, **114**, 96.
13 J. Li, Y. Zhu, R. Ke and J. Hao, *Appl. Catal., B*, 2008, **80**, 202.
14 H. Kannisto, H. H. Ingelsten and M. Skoglundh, *J. Mol. Catal. A: Chem.*, 2009, **302**, 86.
15 V. I. Pârvulescu, B. Cojocaru, V. Pârvulescu, R. Richards, Z. Li, C. Cadigan, P. Granger, P. Miquel and C. Hardacre, *J. Catal.*, 2010, **272**, 92.
16 A. Martínez-Arias, M. Fernández-García, A. Iglesias-Juez, J. A. Anderson, J. C. Conesa and J. Soria, *Appl. Catal., B*, 2000, **28**, 29.
17 K. Shimizu, A. Satsuma and T. Hattori, *Appl. Catal., B*, 2000, **25**, 239.
18 K. Shimizu, J. Shibata, H. Yoshida, A. Satsuma and T. Hattori, *Appl. Catal., B*, 2001, **30**, 151.
19 J. P. Breen and R. Burch, *Top. Catal.*, 2006, **39**, 53.
20 R. Burch, J. P. Breen, C. J. Hill, B. Krutzsch, B. Konrad, E. Jobson, L. Cider, K. Eränen, F. Klingstedt and L. E. Lindfors, *Top. Catal.*, 2004, **30–31**, 19.
21 S. Chansai, R. Burch, C. Hardacre, J. Breen and F. Meunier, *J. Catal.*, 2010, **276**, 49.
22 S. Chansai, R. Burch, C. Hardacre, J. Breen and F. Meunier, *J. Catal.*, 2011, **281**, 98.
23 J. P. Breen, R. Burch, C. Hardacre, C. J. Hill and C. Rioche, *J. Catal.*, 2007, **246**, 1.
24 S. Satokawa, J. Shibata, K. Shimizu, A. Satsuma and T. Hattori, *Appl. Catal., B*, 2003, **42**, 179.
25 J. Shibata, Y. Takada, A. Shichi, S. Satokawa, A. Satsuma and T. Hattori, *J. Catal.*, 2004, **222**, 368.
26 S. Satokawa, J. Shibata, K. Shimizu, A. Satsuma, T. Hattori and T. Kojima, *Chem. Eng. Sci.*, 2007, **62**, 5335.
27 A. Satsuma, J. Shibata, A. Wada, Y. Shinizaki and T. Hattori, *Stud. Surf. Sci. Catal.*, 2003, **145**, 235.
28 J. Shibata, Y. Takada, A. Shichi, S. Satokawa, A. Satsuma and T. Hattori, *Appl. Catal., B*, 2004, **54**, 137.
29 J. Shibata, K.-I. Shimizu, Y. Takada, A. Shichi, H. Yoshida, S. Satokawa, A. Satsuma and T. Hattori, *J. Catal.*, 2004, **227**, 367.
30 P. Baláž, in *Mechanochemistry in Nanoscience and Minerals Engineering*, Springer-Verlag, Berlin Heidelberg, 2008.
31 T. Ishida, N. Kinoshita, H. Okatsu, T. Akita, T. Takei and M. Haruta, *Angew. Chem., Int. Ed.*, 2008, **47**, 9265.
32 T. Ishida, N. Nagaoka, T. Akita and M. Haruta, *Chem.–Eur. J.*, 2008, **14**, 8456.
33 J. Huang, T. Takei, T. Akita, H. Ohashi and M. Haruta, *Appl. Catal., B*, 2010, **95**, 430.
34 J. Huang, E. Lima, T. Akita, A. Guzmán, C. Qi, T. Takei and M. Haruta, *J. Catal.*, 2011, **278**, 8.
35 A. Bruckman, A. Krebs and C. Bolm, *Green Chem.*, 2008, **10**, 1131.
36 A. Lazuen-Garay, A. Pichon and S. L. James, *Chem. Soc. Rev.*, 2007, **36**, 846.
37 K. Ralphs, C. Hardacre and S. L. James, *Chem. Soc. Rev.*, 2013, **42**, 7701.
38 U. Kamolphop, S. F. R. Taylor, J. P. Breen, R. Burch, J. J. Delgado, S. Chansai, C. Hardacre, S. Hengrasmee and S. L. James, *ACS Catal.*, 2011, **1**, 1257.
39 L. F. Gladden and J. Mitchell, *New J. Phys.*, 2011, **13**, 035001.
40 K. M. Song, J. Mitchell, H. Jaffel and L. F. Gladden, *J. Mater. Sci.*, 2010, **45**, 5282.
41 D. Weber, J. Mitchell, J. McGregor and L. F. Gladden, *J. Phys. Chem. C*, 2009, **113**, 6610.
42 J. Mitchell, M. D. Hurlimann and E. J. Fordham, *J. Magn. Reson.*, 2009, **200**, 198.
43 J. P. Korb, *New J. Phys.*, 2011, **13**, 035016.
44 C. D'Agostino, G. L. Brett, P. J. Miedziak, D. W. Knight, G. J. Hutchings, L. F. Gladden and M. D. Mantle, *Chem.–Eur. J.*, 2012, **18**, 14426.
45 C. D'Agostino, T. Kotionova, J. Mitchell, P. J. Miedziak, D. W. Knight, S. H. Taylor, G. J. Hutchings, L. F. Gladden and M. D. Mantle, *Chem.–Eur. J.*, 2013, **19**, 11725.
46 C. D'Agostino, J. Mitchell, L. F. Gladden and M. D. Mantle, *J. Phys. Chem. C*, 2012, **116**, 8975.
47 P. J. McDonald, J. P. Korb, J. Mitchell and L. Monteilhet, *Phys. Rev. E: Stat., Nonlinear, Soft Matter Phys.*, 2005, **72**, 011409.
48 P. J. McDonald, J. Mitchell, M. Mulheron, P. S. Aptaker, J. P. Korb and L. Monteilhet, *Cem. Concr. Res.*, 2007, **37**, 303.
49 A. Abe, N. Aoyamo, S. Sumiya, N. Kakuta and K. Yoshida, *Catal. Lett.*, 1998, **50**, 5.

50 S. Sumiya, M. Saito, H. He, Q. Feng, N. Takezawa and K. Yoshida, *Catal. Lett.*, 1998, **50**, 87.
51 I. Foley, S. A. Farooqui and R. L. Kleinberg, *J. Magn. Reson., Ser. A*, 1996, **123**, 95.
52 F. C. Meunier, J. P. Breen, V. Zuzaniuk, M. Olsson and J. R. H. Ross, *J. Catal.*, 1999, **187**, 493.
53 S. Tamm, H. H. Ingelsten and A. E. C. Palmqvist, *J. Catal.*, 2008, **255**, 304.
54 K. Eränen, F. Klingstedt, K. Arve, L.-E. Lindfors and D. Y. Murzin, *J. Catal.*, 2004, **227**, 328.
55 N. Bion, J. Saussey, M. Haneda and M. Daturi, *J. Catal.*, 2003, **217**, 47.